

Article

Hazard Assessments of Riverbank Flooding and Backward Flows in Dike-Through Drainage Ditches during Moderate Frequent Flooding Events in the Ningxia Reach of the Upper Yellow River (NRYR)

Fuchang Tian, Bin Ma *, Ximin Yuan, Xiujie Wang and Zhichun Yue

State Key Laboratory of Hydraulic Engineering Simulation and Safety, Tianjin University, Tianjin 300350, China

* Correspondence: mabin97@tju.edu.cn; Tel.: +86-22-27401156

Received: 16 April 2019; Accepted: 10 July 2019; Published: 16 July 2019



Abstract: In this study, the riverbank inundation caused by moderate frequent flooding events (with recurrence periods of less than 20 years), along with the increasingly serious hazards of backward flows in dike-through drainage ditches in the Ningxia Reach of the upper Yellow River (NRYR), were investigated. Then, a comprehensive method for hazard assessment of the floodplains and backward flows in the NRYR was proposed, which fully integrated geographical information systems (GISs), remote sensing (RS), and a digital elevation model (DEM), as well as river dynamics theory. This study first established a one-dimensional unsteady hydrodynamic model for the NRYR. The historical flood hydrology observation from 2012, along with the aerial image measurement data of the study area, were used to calibrate and verify the accuracy of the model. The hazards of riverbank inundation and damages to water affected engineering facilities, as well as the backward flows of dike-through drainage ditches caused by the moderate frequent flooding events, were comprehensively analyzed. Also, this study configured the hazard map and proposed revisions to the flood hazard ranking regime definitions, and discussed the impacts and prevention and control measures of moderate frequent flood damages. The proposed method could effectively meet the hazard analysis demands of the moderate frequent flooding events in the NRYR.

Keywords: hazard assessment; moderate frequent flooding events; riverbank inundation; backward flow; dike-through drainage ditches; Ningxia Reach of the upper Yellow River (NRYR)

1. Introduction

Flood disasters are the most devastating, widespread, and frequent natural disasters in human society. From a global perspective, China is one of the countries which suffers the most serious flood disasters. Flood disasters in China affect and restrict the development of both the country's economy and society [1]. The most common flood hazards mainly include rainstorm waterlogging, river channel flooding, dam-burst flooding, dyke breaking, and so on. The hazards of riverbank flooding for wide and shallow rivers are a main form of river channel flood disasters. There are particularly high flooding hazards in the Yellow River bank areas, which are known to be the most prominent. Those areas are characterized by frequent occurrences, serious losses to life and property, and overall high-hazard levels, which have seriously affected the unified planning, construction, and development of the banks. The flood prevention and control measures required in the Yellow River bank areas have become arduous tasks [2]. Therefore, it has become of great significance to conduct hazard analyses and assessments of the Yellow River floodplains.

The flood hazard analysis methods of river floodplain areas mainly include hydraulic, hydrologic, and historical flood disaster methods [3]. Among the aforementioned methods, hydraulic methods

are widely used in the field of flood hazard analysis due to the rigorous approach. These abilities mainly include the applications of one-dimensional hydrodynamic models of river channels [4–8]; two-dimensional hydrodynamic models [2,9–15]; one- and two-dimensional coupling models [16–22]; and three-dimensional hydrodynamic models [23–28]. In a previous related study, Anees et al. discussed the applicability and limitations of one-, two-, and three-dimensional numerical modeling techniques for flood analyses in river channels and floodplains [29]. With the rapid development of spatial information technology, such as geographic information systems (GISs), remote sensing (RS), and global positioning systems (GPSs), a large number of research studies have been recently carried out regarding the application of “3S” technology in flood inundation hazard assessments in river-floodplain areas. These have included flood inundation connectivity and evolution simulations of floodplains or surface flooding based on GIS and digital elevation model (DEM) technology [30–38]; flood hazard analyses and hazard graph mapping based on GIS and hydrodynamic numerical models [39–48]; and flood impact and loss evaluations based on 3S and DEM technology [49–53]. Meanwhile, some researchers have attempted to predict flood inundation hazards in large range or even global scales with low-resolution DEM data and hydrologic and hydrodynamic models [54–58].

In recent years, the research team of the State Key Laboratory of Hydraulic Engineering Simulation and Safety at Tianjin University has completed major research studies regarding the analyses and evaluations of flood hazards in the floodplain areas of the Ningxia-Inner Mongolia Reach of the upper Yellow River. For example, Tian examined the integrated applications of GIS, RS, DEM, hydrodynamic models, and other advanced technologies, and proposed a numerical simulation method of two-dimensional hydrodynamic coupling in river floodplain areas [3]. The method was then applied in order to simulate the joint calculation of the floodplain and dyke-burst flooding in the NRYR. Also, Yuan et al. established a fine-scale hydrodynamic model for flood evolution simulations of the floodplain and dyke-burst flooding in the river-irrigation areas of the Inner Mongolia Reach of the Yellow River, based on a two-dimensional meteorological chromatography theory [15]. In another related study, based on integration technology involving GIS and a hydrodynamic model, Tian et al. formulated a fine-scale hydrodynamic model with actual topography for the simulation and hazard analysis of dyke-burst flooding in the Xiaofeng Ditch of the Yellow River Basin [59]. Wang et al. constructed a spatio-temporal dynamically coupled two-dimensional model for the joint calculation of the flood hazards in the floodplain, burst dykes, and flood protection areas of the Qingshi Reach of the NRYR, using DEM, remote sensing images, and actual measured data. The results provided support for the assessments of the impacts of flooding in the river reach [13]. Wang and Zhang established the one- and two-dimensional coupling model for the NRYR and flood protection zone, and used the powerful data analysis function of GIS to evaluate the impact of super standard flood inundation [60,61].

In accordance with the above analysis, it was determined that the combined applications of GIS and river hydrodynamic models have played important roles in the flood inundation hazard assessments of river channels and floodplains. However, at the present time, “3S” technology is mainly combined with two-dimensional hydrodynamic models in flood inundation hazard analyses of riverbank areas. However, many problems related to two-dimensional fine hydrodynamic river modeling have been found, such as difficulties in terrain acquisition and processing, large numbers of computing grids and iterations, high intensity data processing and storage, long calculation periods, and so on [41]. It is known that during the processes of practical applied research, the advantages of various technologies (for example, the integration of 3S technology and one-dimensional hydrodynamic river modeling) in the hazard analysis and disaster warning and forecasting of river floodplains have not yet been fully exploited. Also, only a few previous research studies have applied these advantages in the analyses and evaluations of the hazards of riverbank inundation and backward flow of dike-through drainage ditches caused by the moderate frequent flooding (with recurrence periods of less than 20 years) of the NRYR. Therefore, in order to solve the problems of the hazard assessments of riverbank inundation caused by moderate frequent flooding and backward flow in dike-through drainage ditches, which have become major concerns in the fields of flood control, damage reduction, river regulation

planning, and flood control evaluations in the NRYR, this study fully integrated GIS, RS, and DEM technologies with a river hydrodynamic model. Then, a hazard simulation model was established for the riverbank inundation caused by moderate frequent flooding and backward flow in dike-through drainage ditches. Finally, this study analyzed and evaluated the hazards caused by moderate frequent flooding with different discharge values in the NRYR, completed a hazard map for the riverbank inundation and backward flow of the moderate frequent flooding on floodplain in the study area, and proposed flood control and damage reduction measures which could potentially address the hazards caused by moderate frequent flooding events.

2. Research Area

The Yellow River is a world famous natural heavy silt-carrying river, with a total length of approximately 5464 km, and a drainage area of approximately 7.52×10^5 km². The Ningxia Reach of the upper Yellow River enters in Ningxia from Nanchangtan of Zhongwei City, and leaves Ningxia from Mahuanggou of Shizuishan City. The Ningxia reach measures 397 km in length, with a drainage area of 5×10^4 km². It passes through a total of 11 cities and counties (districts), as shown in Figure 1. With the completion and utilization of upstream reservoirs in the NRYR, along with changes in the climatic conditions of the area, the relationship between the water and sediment in this river reach has been observed to have been altered, displaying non-coordinated changes. Before the 1980s, the erosion and siltation in the NRYR were basically balanced during many years. The main river channel had the ability to maintain a certain capacity of flood discharge and sediment transport. Then, under the double effects of human activities and natural climate change, the water inflow, sediment transport during flood seasons, and channel-forming peak flows in the NRYR were observed to be greatly reduced. The extensions of the durations of the moderate frequent flooding in the area resulted in the sediment mainly becoming deposited in the main river channel. This has led to increasingly serious deposition and shrinkage of the main river channel, with yearly decreases in the flow on the flat banks, and sharp declines in the water and sediment transport abilities of the NRYR [62,63]. In recent years (particularly in 2012), when the NRYR encountered moderate frequent flooding, the bank areas experienced high inundation hazards. It was found that structures were seriously damaged by flood water, with many dike-through drainage ditches and frequent backward flow phenomenon observed [64]. These factors resulted in the flood control and damage reduction situations becoming increasingly severe. Therefore, the prevention and control of the moderate frequent flooding damages in the NRYR were of particular importance.

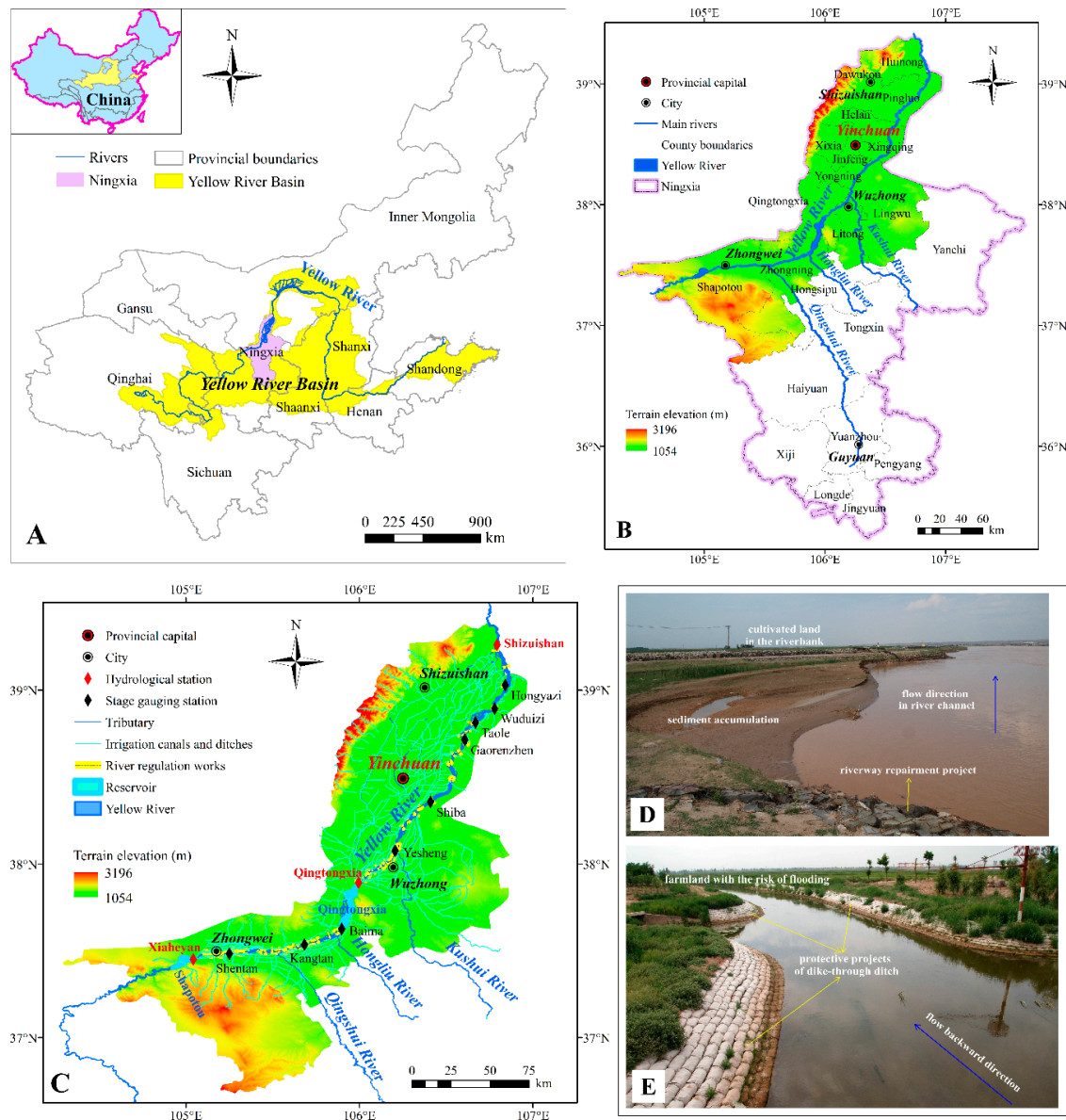


Figure 1. Geographical location map of the research area: (A) Yellow River Basin; (B) Ningxia Hui Autonomous Region; (C) research scope of the Ningxia Reach of the upper Yellow River (NRYR); (D) photos of the main river channel, bank areas, and regulation structure site; (E) actual scene of the typical ditches with backward flow.

3. Data and Methods

3.1. Data

This study’s research data mainly included the topographic data of the river channel in the NRYR, historical flood damage data, and the data of the area’s engineering facilities. All of the data used for the current research study were provided by the Ningxia Water Conservancy. Among these, the basic terrain data mainly included the actual measured river sections of the NRYR during the dry season following the flooding in 2012, high resolution aerial images (1.0 m) in tiff format measured by Yellow River Engineering Consulting Co., Ltd. based on the ADS80 Digital Airborne Sensor manufactured by Leica Geosystems in Switzerland during the same period, and high-precision DEM information with a scale of 1:10000 in grid format derived by the interpolation of Light Detection And Ranging (LiDAR) data based on the PHOTOMOD digital photogrammetry software developed by Racurs in

Russia. The horizontal grid size of DEM is $5\text{ m} \times 5\text{ m}$, and the vertical elevation error is less than 0.22 m. The historical flood damage data mainly included the flood hydrological factors monitored by the hydrological and water level stations along the NRYR in 2012, as well as the flood damage analysis report of 2012. The data from the engineering facilities mainly included the location distribution and design parameters of the dikes, river control structures, and dike danger assessment projects.

3.2. Methods

The geographic information systems (GISs) are information systems with powerful functions, such as geographic spatial data storage, management, analysis, expression, and drawing functions. The GISs have been widely applied and popularized, which has deepened the fields of flood control and damage reduction, as well as water conservancy informatization. Therefore, based on the basic data support of river topography, historical flood damages, and the engineering facilities in the NRYR, this study made full use of many frontier technologies, such as GIS, RS, GPS, DEM, and river hydrodynamic models. A comprehensive method for the hazard assessment of the riverbank inundation caused by moderate frequent flooding and backward flowing in dike-through drainage ditches in the NRYR was proposed in this study. A detailed technical road map is shown in Figure 2.

3.2.1. Basic Multi-Source Data Analysis and Processing

From the perspective of the establishment and validation of this study's hydrodynamic model in the NRYR, and in accordance with the content and format requirements of the different types of data used in this study, a hazard analysis and impact assessment of the moderate frequent flooding, along with a map of the moderate frequent flood hazard analysis and processing were completed for such multi-source data as the river terrain, historical flood damages, and the engineering facilities in the NRYR. Then, based on a GIS platform, this study's main focuses included the following: (1) The formulation of detailed descriptions of the vector information of the main channel (including the linear and planar elements); bank, dike, and dam buttress structures; and historical flood inundation ranges were artificially extracted from the aerial images [65,66], in order to generate a digital line graph for the river channels in the Ningxia Reach of the Upper Yellow River (NRYR); (2) in order to determine the riverbank inundation boundaries of the moderate frequent flooding, a buffering process of the main channel line of rivers was completed. Then, buffered boundary lines with different spacing were obtained. The scattered points having the same spatial distribution characteristics as the flood calculation node of the hydrodynamic river model were arranged along the main channel line of the river and the buffered boundary lines on both sides. Then, the riverbank elevation data which corresponded to all of the scattered points could be extracted based on the GIS and DEM data; (3) in accordance with the numerical calculation results of this study's hydrodynamic river model, the water level elevation attributes were given to the scattered points on the main channel line of the river and the buffered boundary line at both sides, in order to realize the vectorization of the water surface profile of moderate frequent flooding with different discharge values in the NRYR; and (4) the important basic geographic elements in the NRYR were identified and configured, and a hazard map of the moderate frequent flooding in the study area was completed.

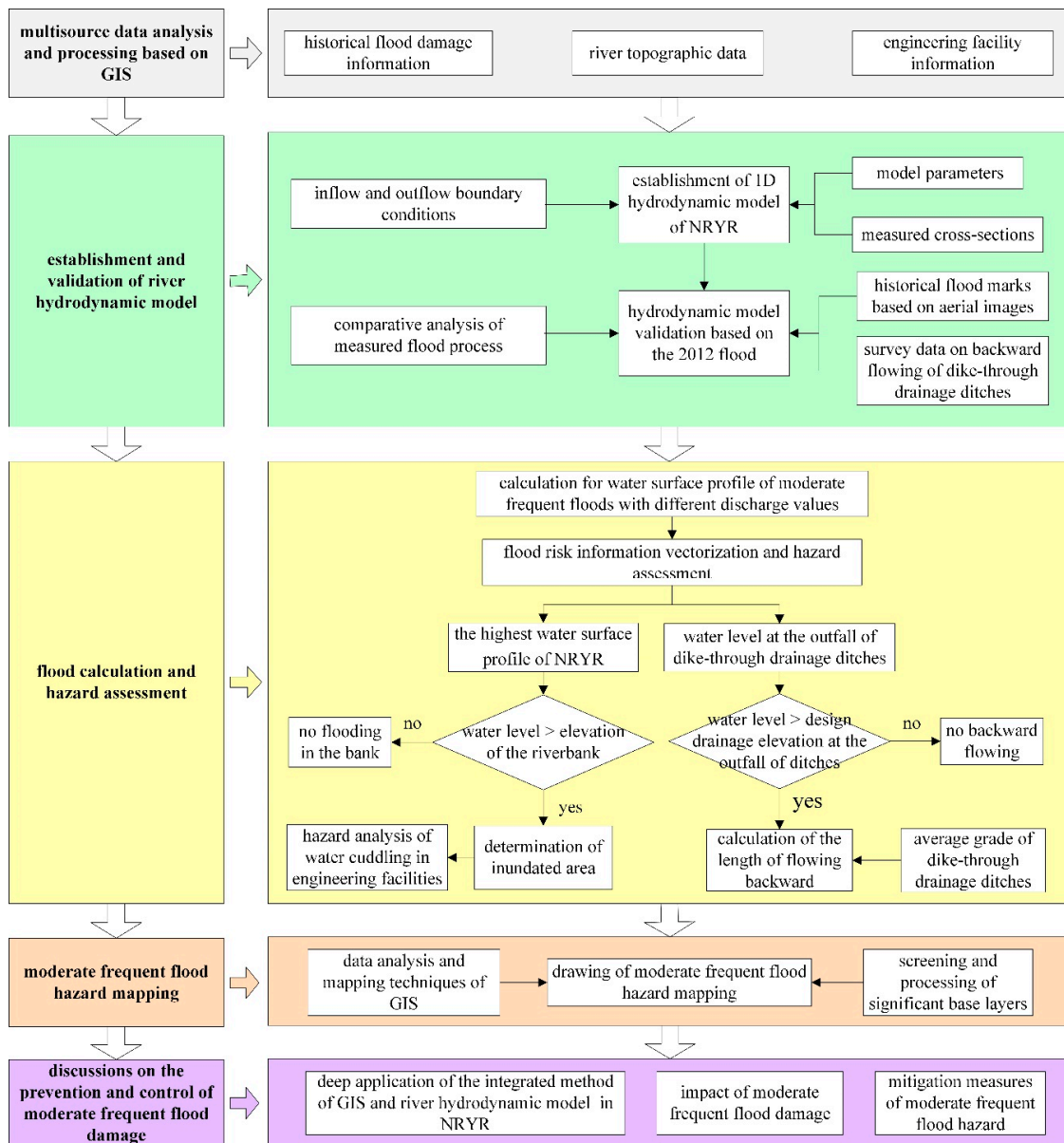


Figure 2. Technical road map for the hazard assessment of riverbank inundation due to moderate frequent flooding and backward flowing in ditches in the NRYR.

3.2.2. Simulation Model of the Flood Evolution in the NRYR

There are three hydrologic stations and one reservoir (Figure 1) in the NRYR, namely Xiaheyan Hydrological Station, Qingtongxia Hydrological Station, Shizuishan Hydrological Station, and Qingtongxia Reservoir. They were considered in this study to be important control nodes of the research range, and used to divide the NRYR into the Weining Reach (from Xiaheyan Hydrological Station to the upstream Baima Stage Gauging Station of the Qingtongxia Reservoir), with a length of 85 km, and the Qingshi Reach (from Qingtongxia Hydrological Station to Shizuishan Hydrological Station), with a length of 191 km. Then, based on the actual measured data of the 69 cross-sections of the NRYR in 2012, a one-dimensional unsteady hydrodynamic model was established for the rivers in the Weining and Qingshi Reaches, with the model control boundary conditions shown in Figure 3. The Saint–Venant equations were employed to describe the flood movement process in a one-dimensional unsteady hydrodynamic model, as shown in Equations (1) and (2), and a 6-point

Abbott scheme was adopted to discretize the control equations. Then, the water level and discharge on the nodes of arranged sections in order were alternately calculated:

$$\frac{\partial Q}{\partial x} + \frac{\partial A}{\partial t} = q, \tag{1}$$

$$\frac{\partial Q}{\partial t} + \frac{\partial \left(\alpha \frac{Q^2}{A} \right)}{\partial x} + gA \frac{\partial Z}{\partial x} + \frac{gQ|Q|}{C^2AR} = 0, \tag{2}$$

where Q is the flash flood discharge in channel (m^3/s), A is the flow area (m^2), x is the distance along the river (m), t is the computing time (s), q represents the discharge per unit width of the interval inflow (m^2/s), R denotes the hydraulic radius (m), C corresponds the Chezy coefficient ($\text{s}/\text{m}^{1/3}$), Z is the water level in channel (m), and α represents the momentum correction factor.

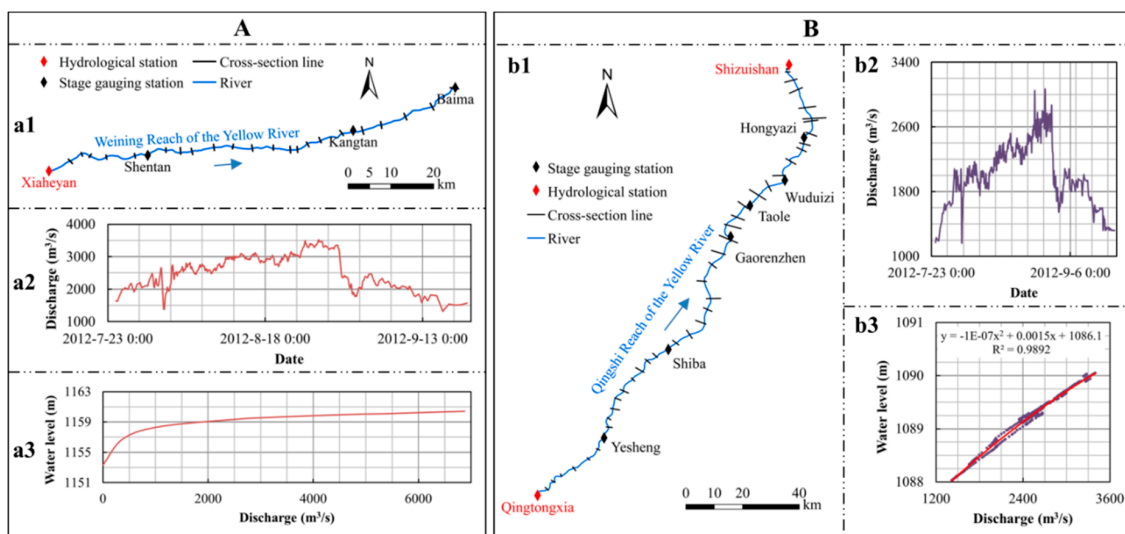


Figure 3. Control conditions of the river hydrodynamic model in the Weining Reach (A) and Qingshi Reach (B) of the NRYR: (a1) Modeling scope of the Weining Reach; (a2) upstream inflow process at Xiaheyuan station; and (a3) water level–flow relationship in the downstream outflow cross-section of the Weining Reach. (b1) Modeling scope of the Qingshi Reach; (b2) upstream inflow process at Qingtongxia station; and (b3) water level–flow relationship in the downstream outflow cross-section of the Qingshi Reach.

In order to ensure the accuracy of the hazard analysis for the moderate frequent flooding events, interpolation and densification treatments were performed on the cross-sections of the river channel. Also, the inflow boundary conditions of the model were that the flow process occurred on the upstream control cross-section (Xiaheyuan and Qingtongxia Hydrological Stations, Figure 3(a2,b2)), while the outflow boundary conditions were the water level–flow relationship on the downstream control cross-section (Baima Stage Gauging Station and Shizuishan Hydrological Station, Figure 3(a3,b3)). At the same time, the water diversion abilities of the main irrigation canals, and the drainage capacities of the ditches on both sides of the rivers, were also considered and treated as source sinking items. The calculation time step of the model was set as 15 s. The comprehensive roughness coefficient of each cross-section was initially set as 0.03, due to the wide and shallow features of the river section. The roughness coefficient value was corrected again when the calibration model for the actual measured data of the flood processes of the NRYR in 2012 were used. The roughness coefficient of the cross-section would be adjusted to a larger value if the measured water level was higher than the calculated result, otherwise the roughness coefficient value would be decreased. The comprehensive

roughness coefficient values of the cross-sections along the NRYR would not be finally determined until the difference between the measured water level and the calculated value could not be reduced.

3.2.3. Flood Hazard Data Information Vectorization and Damage Impact Assessment Method

A one-dimensional hydrodynamic model for the rivers in the NRYR was used to calculate the evolution process of the moderate frequent flooding events with different discharge values, and to extract the water surface profile along the rivers. Then, based on the GIS platform, the cross-section mileage, number and corresponding water level attribute values ($H1$) were assigned to the calculation nodes on the river's center line. A buffering treatment was performed along the river's center line and towards the two river banks at different distances based on the aerial images and DEM. The scattered points displaying the same spacing and quantity were arranged on the buffering line in accordance with the spacing and quantity of the calculation nodes on the river's center line. The same attribute information as the calculation nodes on the river's center line was assigned in order to realize the vectorization of the river's flood hazard information. Then, the terrain elevations of the riverbank ($H2$) and the bottom ($H3$) and top elevations ($H4$) of the engineering facilities at all the scattered points were extracted from the DEM information based on the GIS with the function of "Extract Values to Point". By comparing and analyzing $H1$, $H2$, $H3$, and $H4$, the flood inundation ranges ($H1 \geq H2$) and water related conditions of the engineering facilities in the bank areas were determined as follows: If $H1 \leq H3$, then the structure would not be a water-affected structure; if $H3 < H1 < H4$, the flood waters would reach the structure but not spill over the top of the structure; and if $H1 \geq H4$, the flood waters would spill over the top of the structure. The maximum flood level ($H5$) at the drainage outlet of the main dike-through drainage ditches was extracted from the simulation results of the hydrodynamic river model. When combined with the designed drainage elevation ($H6$) of the dike-through drainage ditches, and the designed gradient of the ditches (i), then the formula, $L = (H5 - H6)/i$, could be used to calculate the backward flow lengths, L , of the flooding in the dike-through drainage ditches along both banks of the Yellow River.

3.2.4. Hazard Map for the Moderate Frequent Flood Damages in the NRYR

In this study, the important digital line graphic layer information was selected and analyzed based on the GIS platform. The classification, combination, diluting, and projection transformation treatments of the layer elements were implemented under a fixed drawing scale. The symbol style, color, size proportion, and display priority of the base layer elements were further adjusted in order to emphasize the expressions of the riverbank inundation scope of the moderate frequent flooding events with different discharge values, lengths of the backward flows in the dike-through drainage ditches, and the conditions of the water-affected structures. The remote sensing image was taken as the background. Then, the hazard map was configured for the moderate frequent flooding events in the NRYR based on a basic principle of comprehensive information and aesthetic appearance.

4. Results

4.1. Calibration and Validation of the Hazard Assessment Model for the Moderate Frequent Flooding Events

Since 1986, the combined storage and regulation of the Longyangxia and Liujiaxia Reservoirs have effectively controlled the flood processes in the NRYR. In 2012, the third flood process with the highest peak discharge was the flood with the largest recorded magnitude since 1986. The actual measured flood discharge of Xiaheyan Hydrological Station was $3520 \text{ m}^3/\text{s}$ (recurrence period: Approximately five years), which was determined to be the most representative of the typical moderate frequent flooding in the NRYR. The riverbank areas and some farmland areas on both sides of the Yellow River were flooded, with multiple dike-through drainage ditches experiencing backward flows. Also, many dangerous situations were observed at dike and dam buttress structures, which threatened the flood control safety of many areas on both sides of the river [67,68]. In this study, by using the

actual measured flood process data of major stage gauging stations in the NRYR during the flood season of 2012, along with the actual measured maximum water levels in the cross-sections along the reach, the calculation accuracy of the proposed one-dimensional hydrodynamic river model could be calibrated. Also, the comprehensive roughness coefficient values of the cross-sections along the Weining and Qingshi Reaches were determined (Figure 4(a3,b3)). The calculated values of the highest water level along the Weining and Qingshi Reaches in 2012 were extracted from the one-dimensional hydrodynamic river model, and the comparative analysis results of the calculated and measured highest water level are shown in Figure 4(a1,b1). Also, the calculation errors of the flood levels along the Weining and Qingshi Reaches are shown in Figure 4(a2,b2). The simulated values of water level changes over time at different stage gauging stations were extracted from the calculation results of the one-dimensional hydrodynamic model, and compared with the measured values, as shown in Figure 5. Then, in order to verify the calculation accuracy of this study’s flood hazard assessment model for the moderate frequent flooding in the NRYR, the riverbank inundation scope, which was determined according to the aerial images (Figure 6A) and survey data of backward flows in dike-through drainage ditches (Figure 6B) after the flooding in 2012, was analyzed through a comparison with the calculation results obtained using this study’s method.

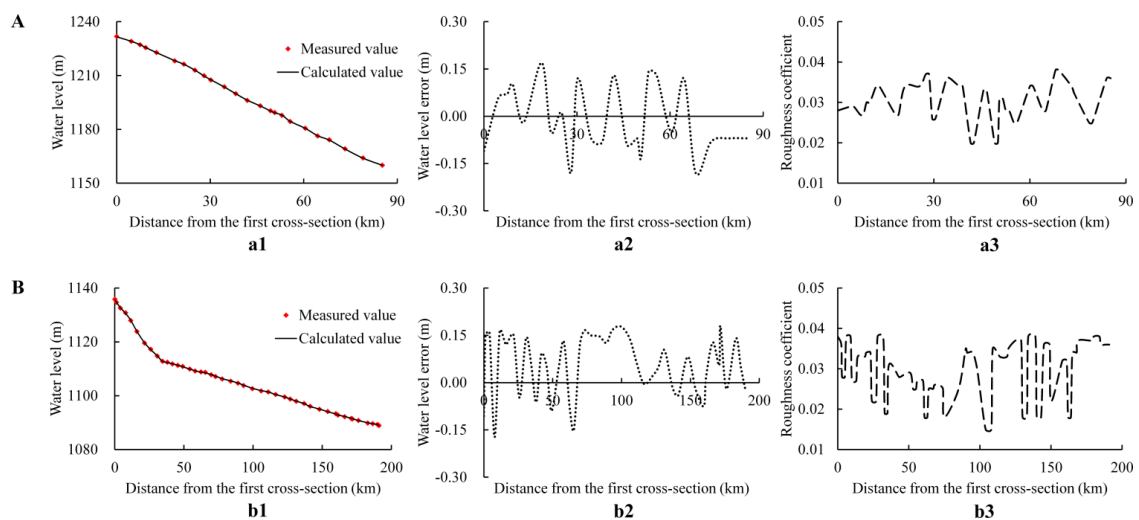


Figure 4. Model calibration of the Weining Reach (A) and Qingshi Reach (B) based on the survey results of the actual measured maximum flood levels in the cross-sections of the NRYR in 2012: (a1,b1) Comparison and analysis of river water surface profile; (a2,b2) calculation errors of the flood levels; (a3,b3) calibration results of the comprehensive roughness coefficient of the cross-sections along the reach.

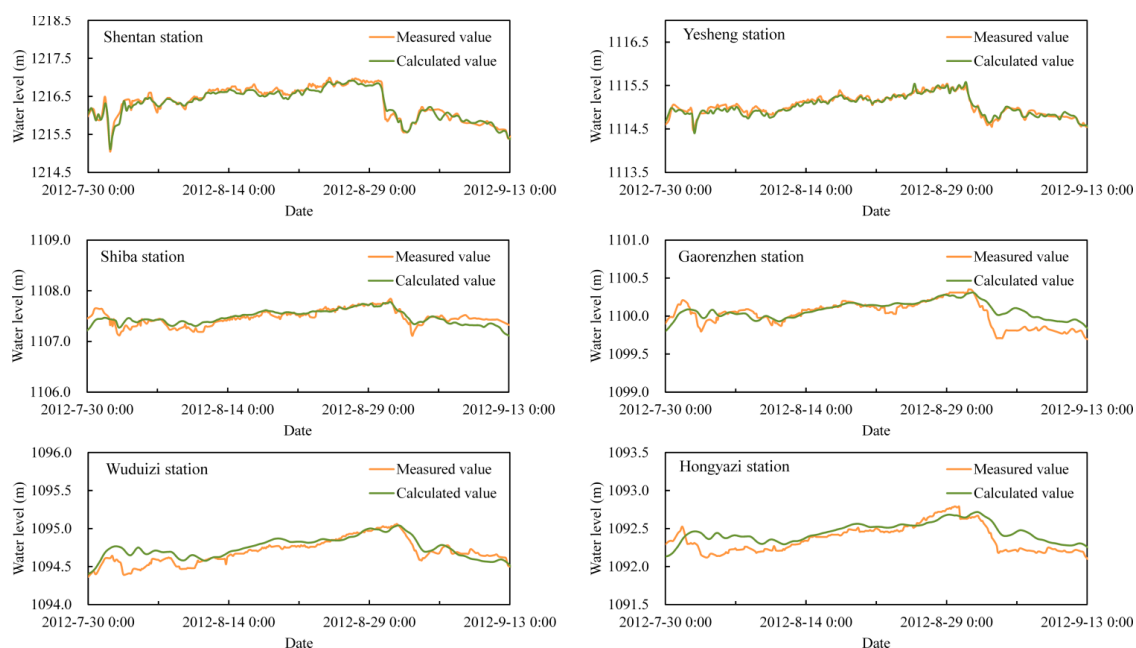


Figure 5. Model calibration based on the actual measured data of the flood processes at the different stage gauging stations of the NRYR in 2012.

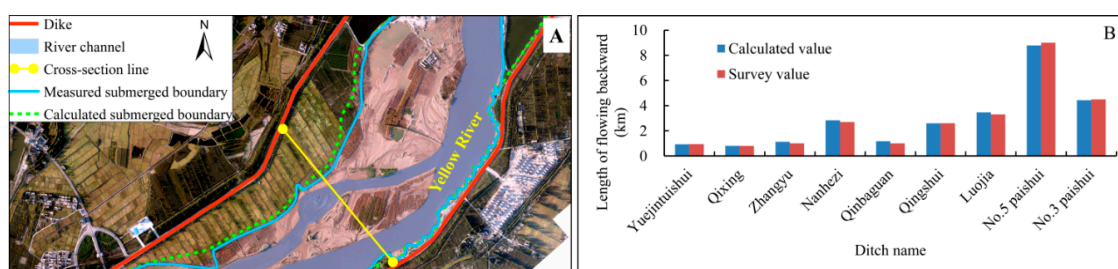


Figure 6. Validation of the moderate frequent flooding hazard assessment results based on the aerial images: (A) Following the flooding events in 2012 and the survey data; (B) backward flowing in the dike-through drainage ditches.

4.2. Evolution Process of the Moderate Frequent Flooding Events with Different Discharge Values

The peak flood discharge with a recurrence period of 20 years at the Xiaheyuan Hydrological Station in the NRYR, which was approved by the Ministry of Water Resources of the People’s Republic of China, is 5660 m³/s. Therefore, in accordance with the local flood control and damage reduction demands, and the actual flood occurrence situations, this research study determined that the moderate frequent flooding events (recurrence period of less than 20 years) with four different analysis magnitudes had flow rates of $Q = 2000, 3000, 4000,$ and $5000 \text{ m}^3/\text{s}$, respectively. Then, based on this study’s calibrated and validated one-dimensional hydrodynamic model for the rivers located in the Weining and Qingshi Reaches, the water surface profiles of the moderate frequent flooding events with different discharge values were calculated. However, due to the calculation length of the river, and the large variations in the upstream and downstream riverbed elevations, the examples of the calculation results of the water surface profiles were given under two working conditions ($Q = 2000 \text{ m}^3/\text{s}$, and $Q = 5000 \text{ m}^3/\text{s}$), in order to improve the display effects, as shown in Figure 7.

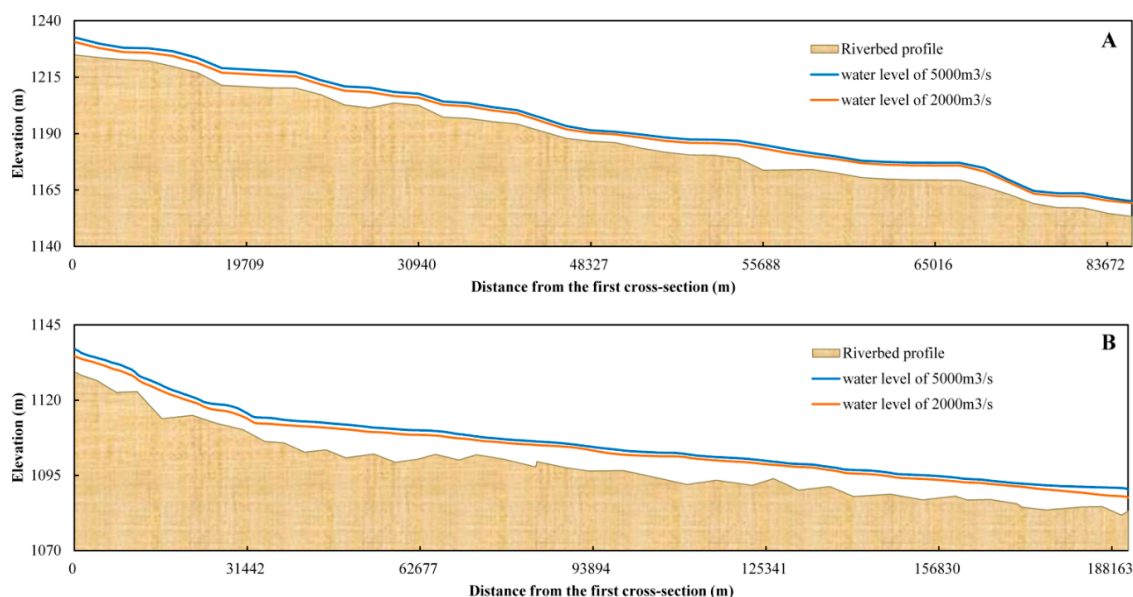


Figure 7. Water surface profiles of the moderate frequent flooding events with different discharge values in the: (A) Weining Reach; and (B) Qingshi Reach of the NRYR.

4.3. Riverbank Inundation Resulting from the Moderate Frequent Flooding and Backward Flows in the Dike-Through Drainage Ditches

4.3.1. Riverbank Inundation Hazard

In this study, in accordance with the calculation results of the water surface profiles for the moderate frequent flooding events with different discharge values, and based on the distributions of the flood water levels on the vectorized cross-sections of the GIS platform, the calculated food levels, riverbank terrain elevations, and design elevations of the engineering facilities at each cross-section were analyzed and compared. The purposes were to determine the water relating scope in the bank areas, and to calculate situations of the flood inundation areas related to the riverbank and water projects. The results are detailed in Table 1.

Table 1. Results of the riverbank inundation hazards resulting from the moderate frequent flooding events in the NRYR.

Reach Name	Hazard Categories	Calculation Conditions of Moderate Frequent Flood			
		Q = 2000 m ³ /s	Q = 3000 m ³ /s	Q = 4000 m ³ /s	Q = 5000 m ³ /s
Weining Reach of the NRYR	Inundated area of bank (km ²)	7.28	10.77	13.99	18.95
	Main water-related engineering facilities	Yixintan, Xingongwan, Shuangqiao, Zhaotan	Nitan, Riverside Water Park in Zhongwei City, Yellow River Wetland Park, Yongfeng, Quanyanshan	Dahegong, Xindun, Yangjiahu, Liuwan, Fengzhuang, Kaigewan, Niding	Cuiyusi, Huangyangwan, Shikongwan, Tiantan, Tongzhuang
Qingshi Reach of the NRYR	Inundated area of bank (km ²)	64.75	107.24	218.68	264.56
	Main water-related engineering facilities	Xiyaozibai, Houwazitan, Sipaikou	Yellow River Ecological Park, Ecological Forest Demonstration Area, Huasan, Donghe, Tonggui, Lihe	Shizuizi Park, Xiabaqing, Beiya, Donglaidian, Toudaodun, Jingxing, Huangsha Ancient Ferry Scenic Area	Jinshui Amusement Park, Changhewan Leisure and Vacation Center, Guangming, Wuxiang, Guanqu

Note: The main water-related engineering facilities refer to the newly added main engineering facilities based on the statistical results of the water-affected structures close to the calculation conditions of the flooding events with lower magnitude.

4.3.2. Backward Flow Hazards of the Dike-Through Drainage Ditches

The flood levels of the dike-through drainage ditches that were significantly affected by the flood control processes in the NRYR were extracted according to the calculation results of the water surface profiles of moderate frequent flooding events with different discharge values. Then, in combination with the designed drainage elevations and average gradients of the dike-through drainage ditches, the lengths of the backward flows in the ditches resulting from the flooding events were comprehensively calculated. This study's analysis process and results are shown in Table 2.

Table 2. Analysis of the lengths of the backward flows in the main dike-through drainage ditches of the NRYR.

Ditch Name	H_0 (m)	i (‰)	Calculation Conditions of Moderate Frequent Flood							
			$Q = 2000 \text{ m}^3/\text{s}$		$Q = 3000 \text{ m}^3/\text{s}$		$Q = 4000 \text{ m}^3/\text{s}$		$Q = 5000 \text{ m}^3/\text{s}$	
			H (m)	L (m)	H (m)	L (m)	H (m)	L (m)	H (m)	L (m)
Yuejintuishui	1201.25	0.82	1201.06	0.00	1201.72	573.17	1202.21	1170.73	1202.56	1597.56
Qixing	1189.62	1.37	1189.80	131.39	1190.42	583.94	1190.90	934.31	1191.23	1175.18
Zhangyu	1175.30	1.46	1176.04	506.85	1176.62	904.11	1177.07	1212.33	1177.44	1465.75
Nanhezi	1158.34	0.98	1160.05	1744.90	1160.68	2387.76	1161.20	2918.37	1161.52	3244.90
Qinbaguan	1126.69	0.53	1126.41	0.00	1126.99	566.04	1127.55	1622.64	1127.94	2358.49
Qingshui	1114.67	0.95	1115.81	1200.00	1116.73	2168.42	1117.23	2694.74	1117.54	3021.05
Luoja	1110.72	0.66	1111.42	1060.61	1112.62	2878.79	1113.10	3606.06	1113.42	4090.91
No. 5 Paishui	1087.56	0.52	1089.75	4211.54	1091.21	7019.23	1092.45	9403.85	1093.17	10,788.46
No. 3 Paishui	1085.68	0.94	1087.78	2234.04	1089.02	3553.19	1090.13	4734.04	1090.49	5117.02

Note: H_0 is the design drainage elevation at the outfall of ditches; i is the design average slope; H is the highest water level at the outfall of ditches; L is the backward flow lengths.

4.4. Map of the Flood Hazards Related to the Moderate Frequent Flood Damages in the NRYR

In accordance with the hazard analysis results of the riverbank inundation caused by the moderate frequent flooding and backward flows in the dike-through drainage ditches in the NRYR, as well as this study's extensive spatial data analysis and geographic mapping function using GIS, a flood hazard map for the moderate frequent flooding in the NRYR was drawn. Consideration was given to highlighting such information as the river systems, dikes, regulation structures, important facilities, inundation scope of the moderate frequent flooding, lengths of the backward flows of dike-through drainage ditches, and so on, as shown in Figure 8.

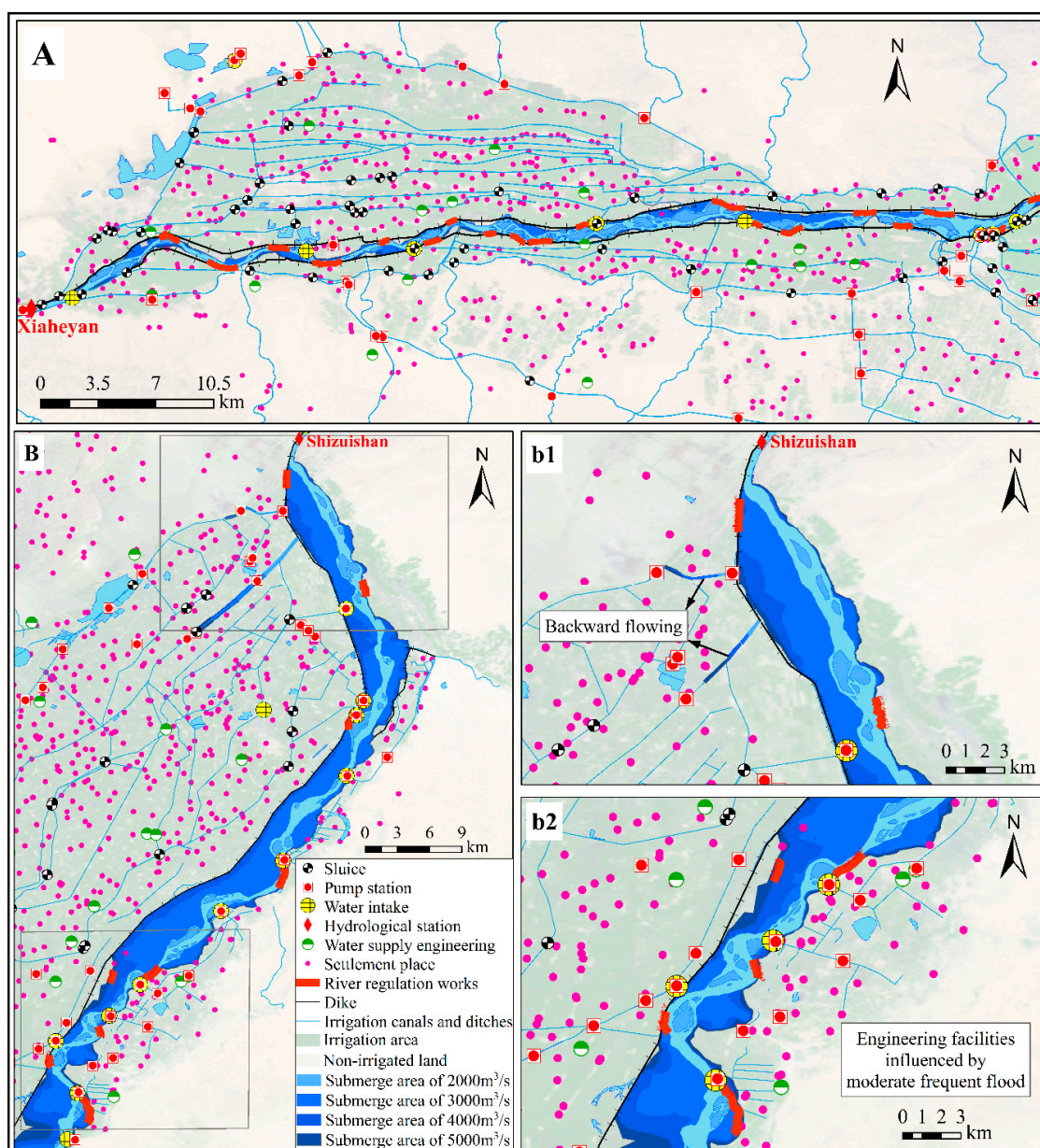


Figure 8. Hazard distribution map of the floodplain and backward flow damages related to the moderate frequent flooding events in local sections of the: (A) Weining Reach and (B) Qingshi Reach of the NRYR; (b1) hazard map of the floodplain and backward flow; (b2) hazard map of the floodplain and water affected engineering facilities.

5. Discussion

5.1. Applications of This Study's Integration Method Using GIS and a River Hydrodynamic Model

This study's one-dimensional hydrodynamic model for the rivers in the Weining and Qingshi Reaches was calibrated and validated on the basis of the actual measured flood processes, and the damage survey data of the NRYR in 2012. As detailed in Figures 4–6, the hydrodynamic model established in this study displayed a high simulation accuracy. The calculation error of the maximum flood level was less than 0.18 m, and there was also a high degree of fitting between the calculated values and actual measured values of the flood processes monitored by each stage gauging station. The value range of the roughness coefficient in the Weining Reach was determined to be between 0.021 and 0.037. Meanwhile, the value of the roughness coefficient in the Qingshi Reach ranged from 0.015

to 0.038. The calculation results of the riverbank inundation range and backward flow lengths of the dike-through drainage ditches were found to be basically consistent with the actual survey data from 2012. Local minor differences of the riverbank inundation area between the calculated and measured value reflected the accumulated errors caused by the terrain, model calculation, and scatter distribution density. The relative calculation errors of the backward flow lengths were $\leq 5.14\%$, and were mainly caused by uncertainties in the water diversion and drainage of the banks during the flood season. As detailed in the analysis results displayed in Figure 7, it was found that the flood water levels of the rivers had gradually decreased from the upper reaches to the lower reaches. It was observed that with the increases of the magnitude of the moderate frequent flood flow, the flood water levels at the same cross-sections displayed a trend of gradually increasing. The calculation results were found to be in line with a trend of topographical relief in the riverbed and the flood movement law in the NRYR. It can be seen that the established model was able to meet the needs of the hazard analyses of the riverbank inundation caused by the moderate frequent flooding events and backward flow of the dike-through drainage ditches in the NRYR. The proposed assessment model could be further verified with the relevant hydrological data of moderate frequent flooding events supplemented and collected to improve its practicability and promotional value.

When compared with other combination methods [3,13,15,41], the integration method of GIS and the one-dimensional hydrodynamic river model has been found to have the advantages of convenient modeling, fast calculation, and high analysis accuracy. This model has been successfully applied to the real-time dynamic decision support systems for flood control and damage reductions in the NRYR [69]. Therefore, it can potentially play an important role in the future hazard prevention and control of moderate frequent flood damages in the study area. With the rapid improvements in computer operation efficiency and parallel computing technology, the next step was to examine one-dimensional (main channel) and two-dimensional (riverbank) hydrodynamic coupling models. At the same time, the water resistance effects of the dikes and regulation structures were considered in order to realize the integrated dynamic simulation of the change in the hazards due to riverbank inundation and water-affected structures over time.

5.2. Hazard Assessments for Riverbank Inundation Caused by the Moderate Frequent Flooding Events and Backward Flows of the Dike-Through Drainage Ditches

As can be seen in Tables 1 and 2, the inundation area, number of water-affected structures, and backward flow lengths of dike-through drainage ditches in the NRYR gradually increased with the increases in the moderate frequent flood flow. Subsequently, the hazards degree also gradually increased. In this study, by taking the minimum flow rate required by the water-affected structures as an important index, the hazard levels of the water related engineering facilities under the same flood effects could be initially judged according to the statistical results, as detailed in Table 1. Then, based on this principle, the engineering facilities with the highest water-related hazard levels in the NRYR were determined. This study's analysis results will potential assist the flood control management department in accurately grasping the key parts and hazard information for flood prevention measures in the NRYR. In Table 2, the lengths of the backward flows of the main dike-through drainage ditches in the NRYR were analyzed and summarized in detail when occurring with the moderate frequent flooding events with different discharge values. Then, by taking the backward flow lengths as the indexes, it was determined that the ditches with high hazards of backward flow mainly included the No. 5 Paishui Ditch, No. 3 Paishui Ditch, and the Luoja, Nanhezi, and Qingshui Ditches. The topographic slopes at both sides of the Qingshi Reach were observed to be gentle, and the ditches had large backward flow lengths. Therefore, the backward flow hazard was determined to be significantly higher than that of the Weining Reach. It is known that backward flows may lead to very serious secondary hazards, such as the inundation resulting from dike overflows or bursts, and erosion damages to canal dike protection structures. The hazard map (Figure 8) for the moderate frequent flood damages in the NRYR intuitively showed the hazards to the floodplain, backward flows, and water-affected structures

caused by the moderate frequent flooding events with different discharge values. These findings can potentially provide support for the protection of engineering facilities, flood-fighting and emergency rescue efforts, and flood risk management procedures in the future.

The Liujiaxia Reservoir was integrated with the Longyangxia Reservoir to regulate and control the water and sediment of its downstream channel, including the NRYR, since 1986. Since 1998, the construction of a river dike and regulation structures in the NRYR were implemented in different construction scales. These actions effectively controlled the regime shifting of the river, as well as scouring damages of the banks on both sides of the river. However, the river sedimentation situation had still not been thoroughly resolved [63]. The analysis of the combined results of the typical cross-sections in the NRYR (Figure 9) revealed that since 1993, the riverbed elevation in the NRYR has been silting and uplifting year by year overall. Also, the main channel displayed a high degree of shifting and swinging, which seriously reduced the flood carrying capacity of the river channel. Figure 10 shows the changing processes of the maximum monthly mean average runoff at Xiaheyan Hydrological Station of the NRYR during the period ranging from 1986 to 2013. The flood which occurred in 2012 was a moderate frequent flooding event, with the largest recorded magnitude since 1986. As can be seen in Figure 9, the flooding which occurred in 2012 played an important role in the channel scouring and shaping of an effective flood carrying river. However, it also caused a high degree of shifting in the main channel. Therefore, under the combined regulation effects of the Longyangxia and Liujiaxia Reservoirs, it was observed that there is an extremely high frequency of moderate frequent flooding events with lower magnitudes in the NRYR. Moreover, the inharmonious water and sediment relationships have led to the yearly sedimentation of the riverbed, in turn resulting in yearly increases in the potential flood hazards. In the cases of moderate frequent flooding events with high magnitudes in the NRYR, high hazards of riverbank inundation and backward flows in dike-through drainage ditches would be evident, as well as potential damages to water related engineering facilities. However, with the entire river in a scouring state, as indicated by the scouring of the main channel and bank sedimentation, the conditions would be conducive to shaping an effective flood and sediment discharging channel, thereby maintaining the healthy and sustainable development of the rivers. In the cases of moderate frequent flooding events with low magnitudes, the hazard levels for the riverbank inundation, backward flows in dike-through drainage ditches, and damages to water related engineering facilities would be lower. However, the main river channel and banks would be in sedimentation states, and the entire riverbed would become raised, which would not be conducive to the healthy and sustainable development of the rivers in the long term. Therefore, there should be an appropriate magnitude for the moderate frequent flooding events, which not only would maintain the basic stability of the river morphology in the NRYR but also minimize the flood hazards [70,71]. In summary, seeking an optimal critical flow was an important part of the next research step.

It is worth noting that the flood process in the NRYR changed greatly after 1986, due to the combined regulation and control of the Longyangxia and Liujiaxia Reservoirs. According to the statistical analysis of the occurrence frequency of flood peak flow of Xiaheyan Hydrological Station, in nearly 30 years after 1986, the flood peak flow corresponding to recurrence periods of 20 years is 3649 m³/s, which was reduced by 2011 m³/s, compared with the 5660 m³/s approved by the Ministry of Water Resources of the People's Republic of China. This shows that the construction and application of the Longyangxia Reservoir resulted in a greatly reduced runoff in the NRYR, and it is necessary to recheck and correct the current design flood approval results based on the actual hydrological data statistics results to reasonably guide the river engineering design and its impact evaluation.

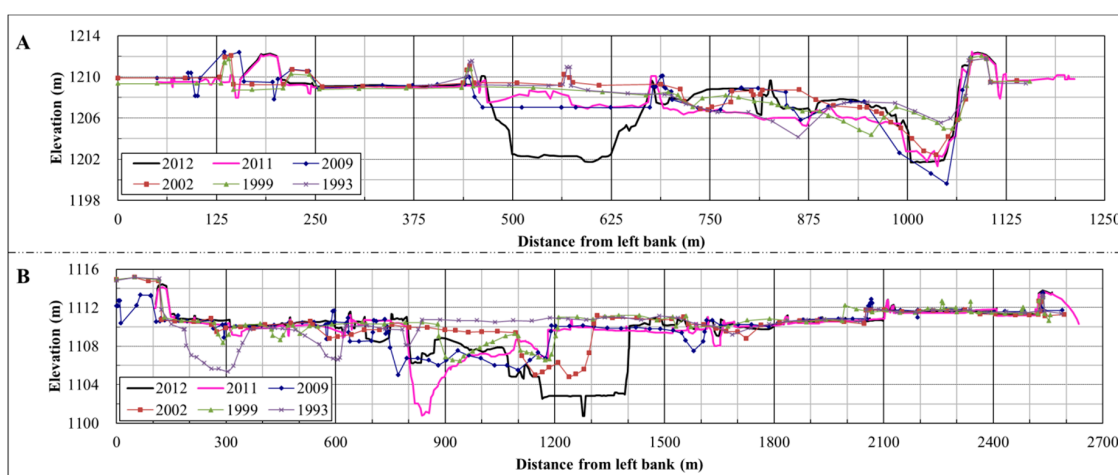


Figure 9. Combined graphs for the actual measured multi-year cross-sections at certain locations in the: (A) Weining Reach; and (B) Qingshi Reach of the NRYR.

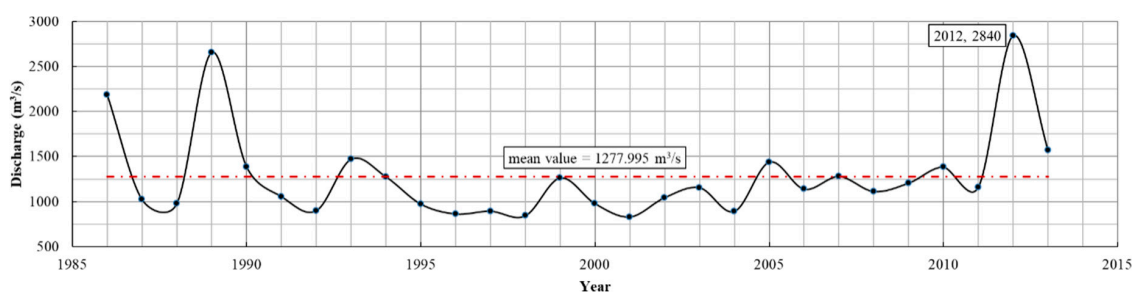


Figure 10. Actual measured maximum monthly mean discharge levels of the Xiaheyan Hydrological Station in the NRYR over time.

5.3. Potential Impacts on the Study Area of Moderate Frequent Flooding Damages

The NRYR has been suffering from the cross-effects of moderate frequent flooding with different discharge values for a long period of time. This has led to a high degree of swinging and shifting in the main river channel [64]. The sediment deposition has raised the elevation of the riverbed, resulting in higher water levels under flooding conditions with the same magnitude. This developmental trend will potentially cause major threats to the regional ecological environment, as well as the safety of the local water supply. Also, the management of flood control may be impacted, which will seriously influence the regional water environment, including the ecology and safety of the water; bank farming and farmland landscapes; safety of the water diversion pumping stations and diversion canal systems; and the safety of residents and properties on both sides of the Yellow River. Furthermore, the constructions in the economic belt and ecological landscape corridor in the NRYR will be seriously restricted.

5.3.1. Impacts on the Coastal Water Diversion Projects

Figure 11 shows the distribution of the engineering facilities (such as the water sluice, water intake, water diversion pumping station, water diversion canal system, water supply works, and so on) in the irrigation area along the banks on both sides of the NRYR. It was found that, under the effects of moderate frequent flooding for a long period of time, the changes in the main flow paths of the rivers in the NRYR have led to flow separations in the water intake on both sides of the Yellow River. Also, water breaking and shortage phenomena were observed in the water source areas, which tend to influence the normal irrigation processes of the local farmlands, and the safety of the local water supply from the Yellow River. Moreover, long-term water supply safety problems will also cause a series of social problems. The sediment deposition has resulted in the raised elevation of the main

channel and bank areas, leading to a raised terrain in the water source areas on both sides of the Yellow River. The water intake of the diversion canals and pumping stations then becomes easily covered by sediment deposition, which renders the diversion more difficult. It also affects the safety of the water intake and diversion canal system, reduces the water transportation capacity of the projects, and restricts farmland irrigation and water supply safety in the Yellow River region.

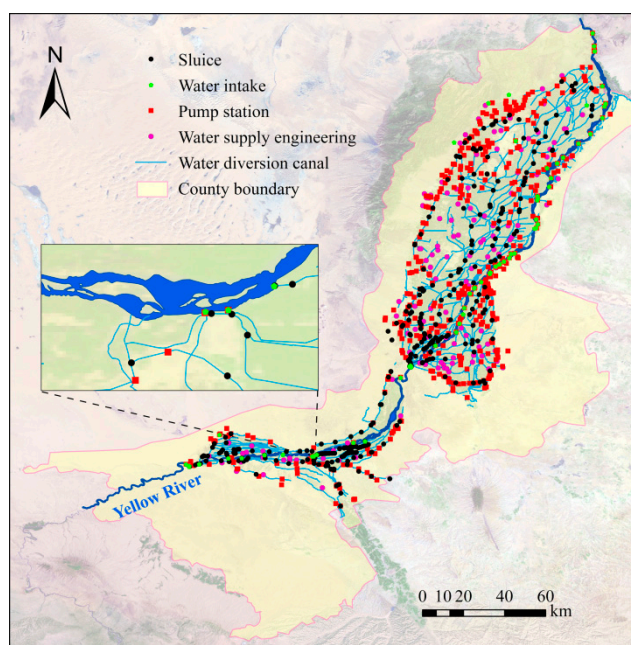


Figure 11. Distribution of the engineering facilities in the irrigation areas along both banks of the NRYR.

5.3.2. Impacts on the River Regulation Structures

When moderate frequent flooding events occur in the NRYR, the mainstream tends to rush into the riverbed from time to time, which causes serious destruction of the dikes and danger control structures. These factors present potential hazards of dike bursts, along with significant losses of life and property, and aggravate the severity of the regional flood controls. At the same time, the floodplains and shifting of the main river channel will potentially cause a major loss of farmland, and destruction of river regulation structures on the banks.

5.3.3. Impacts on the Ecological Environments of the Rivers

The irregular shifting of main river channel in the NRYR has led to the redistribution of the river channel and banks, and has changed the regimen of the river, disturbed the surface, and destroyed many plants. This has subsequently led to the reduction of zooplankton and phytoplankton in the water and benthic biomass, and has caused the migration of the spawning, feeding, and over-wintering grounds of the local fish. At the same time, the sedimentation of the river, as well as the shifting of the main channel, has led to reductions in farmland planting areas on the banks, and serious destruction of the healthy and sustainable development of the ecological water environment in the NRYR.

5.4. Flood Control and Damage Reduction Measures against Moderate Frequent Flooding in the NRYR

The NRYR has the characteristics of abundant sediment, frequent floodplains from moderate frequent flooding events, high hazards for the backward flows of dike-through drainage ditches, and serious losses resulting from flooding damages. In order to further reduce the backward flows caused by the moderate frequent flooding, reduce the potential sediment deposition hazards on the banks, promote the healthy and sustainable development of the NRYR, and guarantee the planning

and construction of the economic belt along the Yellow River, this study mainly proposed flood control and damage reduction measures against moderate frequent flooding events from the perspective of the construction of flood control engineering and flood risk management. This study referenced to the research results regarding flood control and damage reduction measures in the bank of the lower reaches of the Yellow River [72,73]. The recommendations of this study are as follows: (1) An optimization of the regulation scheme for the upstream reservoir, reasonable control of the water and sediment inflow conditions in the NRYR, and reductions in the probability of riverbank inundation. These would result in shaping a favorable geomorphology for the river channel, thereby improving the capacity of the flood and sediment discharge. (2) The construction of river regulation structures should be continually strengthened in the NRYR, and the swinging of the main channel and bank erosion caused by moderate frequent flooding should be effectively controlled. (3) Gate control measures for the dike-through drainage ditches should be constructed, slope protection for bank ditches should be strengthened, and the dikes in the area should be made thicker, in order to improve the scour resistance abilities of the drainage systems, and decrease the hazards of backward flows, overflows, and inundation caused by flooding events. (4) The safety constructions in the bank areas should be strengthened, with emergency flood escape systems and escape roads constructed. Also, flood control contingency plans need to be formulated for the study area. (5) A decision support system for flood control in the NRYR should be established, in order to realize the real-time warning and forecasting of floods, and rapid decision making for flood control and damage reductions. Doing so would further improve the levels of flood risk management and reduce flood hazards and potential losses in the NRYR.

6. Conclusions

(1) This research study proposed a hazard assessment method, which was applicable to the riverbank overflowing and inundation caused by moderate frequent flooding and backward flows of dike-through drainage ditches in the NRYR based on the combination of GIS, RS, DEM, and a hydrodynamic river model. It was found that this method could potentially be applied to provide technical support for moderate frequent flood risk analysis and damage prevention in the NRYR.

(2) This study established a hazard analysis model for the floodplains caused by moderate frequent flooding events and backward flows of dike-through drainage ditches in the NRYR. The calibration and validation of the established model were conducted using the actual measured flood process data from 2012, as well as the damage survey information and aerial image data, which guaranteed the accuracy of the model's analysis and calculations. Also, the hazards of the floodplains caused by moderate frequent flooding events with different discharge values, and backward flows of dike-through drainage ditches in the NRYR could be more accurately evaluated using the proposed method. A hazard map for the moderate frequent flood damages was mapped based on the GIS platform. The results showed that, under the influences of the year-by-year increases in the sedimentation of the riverbed in the NRYR, the rise in the moderate frequent flooding levels had led to frequent occurrences and higher hazards of backward flow phenomena in the bank areas, which should be drawn to the attention of the flood prevention department for the study area. The calculation results provided the hazard information of moderate frequent flooding events with different discharge values, including damages to water related engineering facilities and the backward flows of dike-through drainage ditches, which were of certain reference value for local water conservancy and flood control departments.

(3) In order to ensure the healthy and sustainable development of the rivers in the NRYR, and also promote the development of the economic belts on both sides of the river, flood control and damage reduction measures for moderate frequent flooding were proposed in this study, which may have some guiding significance in the NRYR. The aforementioned measures were presented from the perspective of the construction of flood control structures and flood risk management processes, based on the in-depth analysis and assessment of the moderate frequent flood hazards and influences in the NRYR.

Author Contributions: Conceptualization, X.Y. and B.M.; methodology, X.Y. and F.T.; software, F.T.; validation, F.T. and X.W.; formal analysis, F.T.; investigation, Z.Y.; resources, X.W.; data curation, F.T.; writing—original draft preparation, Z.Y.; writing—review and editing, F.T. and B.M.; visualization, B.M.; supervision, X.Y.; project administration, X.Y.; funding acquisition, X.Y.

Funding: This research was funded by National Key R&D Program of China, grant number 2018YFC1508403; Science Fund for Creative Research Groups of the National Natural Science Foundation of China, grant number 51621092; Program of Introducing Talents of Discipline to Universities, grant number B14012; and Fund for Key Research Area Innovation Groups of China Ministry of Science and Technology, grant number 2014RA4031.

Acknowledgments: Thanks are given to Libing Guo and Yan Yang of the Ningxia Water Conservancy for their supply of data and research ideas pertaining to this study. We would also like to express our sincere gratitude to the anonymous reviewers for their helpful comments.

Conflicts of Interest: The authors declare no conflict of interest. The funders had no role in the design of the study; in the collection, analyses, or interpretation of data; in the writing of the manuscript, or in the decision to publish the results.

References

- Zuo, H.; Yan, Y.; Zhang, S.; Chen, Y.; Chen, M.; Sun, B.; Zhang, Y. Record of major flood and waterlogging disasters prevention since 1949 in China. *China Flood Drought Manag.* **2009**, *29*, 20–38. (In Chinese)
- Zhang, X.; Xia, J.; Li, N. Impacts of mesh scale and village region roughness on predictions of flood inundation over complex floodplains. *J. Hydroelectr. Eng.* **2016**, *35*, 48–57. (In Chinese)
- Tian, F. Numerical Simulation of 2D Coupling Hydrodynamic Model of River Channel-Flood Plain Two-Dimensional and Its Application in Flood Risk Analysis. Master's Thesis, Tianjin University, Tianjing, China, 2014. (In Chinese)
- Panda, R.K.; Pramanik, N.; Bala, B. Simulation of river stage using artificial neural network and MIKE 11 hydrodynamic model. *Comput. Geosci.* **2010**, *36*, 735–745. [[CrossRef](#)]
- Mohammadi, S.A.; Nazariha, M.; Mehrdadi, N. Flood damage estimate (quantity), using HEC-FDA Model. Case study: The Neka River. *Procedia Eng.* **2014**, *70*, 1173–1182. [[CrossRef](#)]
- Merkuryeva, G.; Merkurjev, Y.; Sokolov, B.V.; Potryasaev, S.; Zelentsov, V.A.; Lektuers, A. Advanced river flood monitoring, modelling and forecasting. *J. Comput. Sci.* **2015**, *10*, 77–85. [[CrossRef](#)]
- Pearson, A.J.; Pizzuto, J. Bedload transport over run-of-river dams, Delaware, USA. *Geomorphology* **2015**, *248*, 382–395. [[CrossRef](#)]
- Shelley, J.; Gibson, S.; Williams, A. Unsteady flow and sediment modeling in a large reservoir using HEC-RAS 5.0. In Proceedings of the 2005 Federal Interagency Sediment Conference, Reno, NV, USA, 19–23 April 2015.
- Dai, B.T.; Mussetter, R.A.; Boberg, S.A. FLO-2D modeling to support the Rio Grande Bosque restoration feasibility study, Albuquerque reach of the middle Rio Grande, New Mexico. In Proceedings of the World Environmental and Water Resources Congress, Albuquerque, NM, USA, 20–24 May 2012; pp. 2593–2602.
- Adegbe, M.; Alkem, D.; Jetten, V.G.; Agbor, A.T.; Abdullahi, I.N.; Shehu, O.U.; Unubi, A.S. Post seismic debris flow modelling using Flo-2D; case study of Yingxiu, Sichuan Province, China. *J. Geogr. Geol.* **2013**, *5*, 101–115.
- Yu, C.; Duan, J. Two-dimensional hydrodynamic model for surface-flow routing. *J. Hydraul. Eng.* **2014**, *140*, 04014045. [[CrossRef](#)]
- Lanni, C.; Mazzorana, B.; Macconi, P.; Bertagnolli, R. Suitability of mono-and two-phase modeling of debris flows for the assessment of granular debris flow hazards: Insights from a case study. In *Engineering Geology for Society and Territory*; Springer International Publishing: Cham, Switzerland, 2015; Volume 2, pp. 537–543.
- Wang, X.; Wang, L.; Tian, F.; Yuan, X. Two-dimensional flood calculation model of overflow, levee breach and flood control protected area based on spatiotemporal dynamic coupling. *J. Nat. Disasters* **2015**, *24*, 57–63. (In Chinese)
- Yuan, X.; Tian, F.; Feng, G.; Wang, L. Two-dimensional hydrodynamic model and its application of levee-breach flood. *South North Water Transf. Water Sci. Technol.* **2015**, *13*, 225–230. (In Chinese)
- Yuan, X.; Tian, F.; Wang, L. Comprehensive two-dimensional associate hydrodynamic models for overflow and levee-breach flood and its application. *Adv. Water Sci.* **2015**, *26*, 83–90. (In Chinese)

16. Dutta, D.; Alam, J.; Umeda, K.; Hayashi, M.; Hironaka, S. A two-dimensional hydrodynamic model for flood inundation simulation: A case study in the lower Mekong river basin. *Hydrol. Process.* **2007**, *21*, 1223–1237. [[CrossRef](#)]
17. Lin, B.; Falconer, R.A.; Liang, D. Linking one-and two-dimensional models for free surface flows. *Water Manag.* **2007**, *160*, 145–151.
18. Li, D.; Lin, Y.; Zhou, Z. Research on 1D and 2D numerical simulation of flood routing and its application of combined-regulation in detention basin. *Eng. Sci.* **2010**, *12*, 82–89. (In Chinese)
19. Zhang, D.; Li, D.; Chen, Z.; Wang, X. Coupled one-and two-dimensional hydrodynamic models for levee-breach flood and its application. *J. Hydroelectr. Eng.* **2010**, *29*, 149–154. (In Chinese)
20. Benjankar, R.; Tonina, D.; Mckean, J. One-dimensional and two-dimensional hydrodynamic modeling derived flow properties: Impacts on aquatic habitat quality predictions. *Earth Surf. Process. Landf.* **2014**, *40*, 340–356. [[CrossRef](#)]
21. Yuan, X.; Pang, J.; Tian, F.; Li, C. Application of multi-breach river network coupling model in flood analysis of flood control protection zone. *J. Water Resour. Water Eng.* **2016**, *27*, 128–135. (In Chinese)
22. Yuan, X.; Xue, W.; Feng, G.; Li, C. A coupled one-and two-dimensional hydrodynamic model for analysis of levee-breach flood and its application. *Adv. Sci. Technol. Water Resour.* **2016**, *36*, 53–58. (In Chinese)
23. Stoesser, T.; Wilson, C.; Bates, P.; Dittrich, A. Application of a 3D numerical model to a river with vegetated floodplains. *J. Hydroinform.* **2003**, *5*, 99–112. [[CrossRef](#)]
24. Andersson, L.; Blue, P.; Nicolas, J.P. Calibration of numerical models for small debris flows in Yosemite Valley, California, USA. *Nat. Hazards Earth Syst. Sci.* **2005**, *5*, 993–1001.
25. Yuan, P.; Zhang, J.; Duan, H.; Liu, P. Study on the calculation of the flood around the village platform at beach in the lower reaches of the Yellow River. *Yellow River* **2009**, *31*, 104–109. (In Chinese)
26. Toombes, L.; Chanson, H. Numerical limitations of hydraulic models. In Proceedings of the 34th IAHR World Congress, 33rd Hydrology and Water Resources Symposium and 10th Conference on Hydraulics in Water Engineering, Brisbane, Australia, 26 June–1 July 2011; Engineers Australia: Barton, Australia, 2011; pp. 2322–2329.
27. Li, C. Numerical Investigation of a hybrid wave absorption method in 3D numerical wave tank. *Comput. Model. Eng. Sci.* **2015**, *107*, 125–153.
28. Li, C.; Campbell, B.K.; Liu, Y.; Yue, D.K.P. A fast multi-layer boundary element method for direct numerical simulation of sound propagation in shallow water environments. *J. Comput. Phys.* **2019**, *392*, 694–712. [[CrossRef](#)]
29. Anees, M.T.; Abdullah, K.; Nawawi, M.N.M.; Rahman, N.N.N.A.; Piah, A.R.M.; Zakaria, N.A.; Syakir, M.I.; Omar, A.K.M. Numerical modeling techniques for flood analysis. *J. Afr. Earth Sci.* **2016**, *124*, 478–486. [[CrossRef](#)]
30. Wan, H.; Zhou, C.; Wan, Q.; Wang, C. The construction of flood routing model supported by GIS Technology. *Geogr. Res.* **2001**, *20*, 407–415. (In Chinese)
31. Ding, Z.; Li, J.; Li, L. Method for flood submergence analysis based on GIS grid model. *J. Hydraul. Eng.* **2004**, *35*, 56–60.
32. Liu, Y.B.; Smedt, F.D. Flood modeling for complex terrain using GIS and remote sensed information. *Water Resour. Manag.* **2005**, *19*, 605–624. [[CrossRef](#)]
33. Zhang, Y.; Dong, J.; Han, M. Research of flood routing simulation system based on GIS. *Chin. J. Sci. Instrum.* **2006**, *27*, 936–937. (In Chinese)
34. Merwade, V.; Cook, A.; Coonrod, J. GIS techniques for creating river terrain models for hydrodynamic modeling and flood inundation mapping. *Environ. Model. Softw.* **2008**, *23*, 1300–1311. [[CrossRef](#)]
35. Chen, K. Research and implementation of GIS-based flood assessment system. *J. Catastrophol.* **2009**, *24*, 35–39. (In Chinese)
36. Zhang, D.H.; Liu, R.; Zhang, Y.X.; Xie, J.H. The design and implement of a new algorithm to calculate source flood submerge area based on Dem. *J. East China Inst. Technol.* **2009**, *32*, 181–184. (In Chinese)
37. Chen, Y.; Wang, B.; Pollino, C.A.; Cuddy, S.M.; Merrin, L.E.; Huang, C. Estimate of flood inundation and retention on wetlands using remote sensing and GIS. *Ecohydrology* **2014**, *7*, 1412–1420. [[CrossRef](#)]
38. Teng, J.; Vaze, J.; Dutta, D.; Marvanek, S. Rapid inundation modelling in large floodplains using LiDAR DEM. *Water Resour. Manag.* **2015**, *29*, 2619–2636. [[CrossRef](#)]

39. Li, N.; Cheng, X.; Yuan, X.; Hu, C. Development of Shanghai flood risk mapping and information query system. *Water Resour. Manag.* **2002**, *2*, 48–49. (In Chinese)
40. Sinnakaudan, S.K.; Ghani, A.A.; Ahmad, M.S.S.; Zakaria, N.A. Flood risk mapping for Pari River incorporating sediment transport. *Environ. Model. Softw.* **2003**, *18*, 119–130. [[CrossRef](#)]
41. Zhu, Q. Research of 2D Water and Sediment Numerical Modeling Based on GIS and Its Application in the Lower Yellow River. Ph.D. Thesis, Hohai University, Nanjing, China, 2005. (In Chinese)
42. Wei, Y.; Yao, B.; Xin, G.; Yang, H. Application of ArcGIS in flood risk map system of Yellow River beach area. *Yellow River* **2009**, *31*, 99. (In Chinese)
43. Fu, C.; Yuan, X.; Yang, M. A real-time dynamic coupling model for flood routing and its application to flood risk charting. *Hydro-Sci. Eng.* **2013**, *5*, 32–38. (In Chinese)
44. Patra, J.P.; Kumar, R.; Mani, P. Combined fluvial and pluvial flood inundation modelling for a project site. *Procedia Technol.* **2016**, *24*, 93–100. [[CrossRef](#)]
45. Yuan, X.; Tian, F. *Research on the Flood Analysis and Risk Mapping of Flood-Protected Area in the Ningxia Reach of Yellow River*; China Water & Power Press: Beijing, China, 2016. (In Chinese)
46. Mentzafou, A.; Markogianni, V.; Dimitriou, E. The use of geospatial technologies in flood hazard mapping and assessment: Case study from River Evros. *Pure Appl. Geophys.* **2017**, *174*, 679–700. [[CrossRef](#)]
47. Vu, T.T.; Ranzi, R. Flood risk assessment and coping capacity of floods in central Vietnam. *J. Hydro-Environ. Res.* **2017**, *14*, 44–60. [[CrossRef](#)]
48. Mohammed, M.P. Flood hazard zoning of Tarlac City: Towards the development of flood overlay zones and provision. *Procedia Eng.* **2018**, *212*, 69–76. [[CrossRef](#)]
49. Li, G. Flood loss assessment technique and its application based on GIS. *Geogr. Geo-Inf. Sci.* **2003**, *19*, 97–100. (In Chinese)
50. Qin, N.; Jiang, T. GIS based risk zoning and assessment of flood disaster in the middle and lower reaches of the Yangtze River Basin. *J. Nat. Disasters* **2005**, *14*, 1–7. (In Chinese)
51. Yuan, X. The application of modern information technology in flood control and disaster reduction. *China Flood Drought Manag.* **2010**, *20*, 24–27. (In Chinese)
52. Ntajal, J.; Lamptey, B.L.; Mahamadou, I.B.; Nyarko, B.K. Flood disaster risk mapping in the Lower Mono River Basin in Togo, West Africa. *Int. J. Disaster Risk Reduct.* **2017**, *23*, 93–103. [[CrossRef](#)]
53. Yousefi, S.; Mirzaee, S.; Keesstra, S.; Surian, N.; Pourghasemi, H.R.; Zakizadeh, H.R.; Tabibian, S. Effects of an extreme flood on river morphology (case study: Karoon River, Iran). *Geomorphology* **2018**, *304*, 30–39. [[CrossRef](#)]
54. Dai, Y.; Kanae, S.; Kim, H.; Oki, T. A physically based description of floodplain inundation dynamics in a global river routing model. *Water Resour. Res.* **2011**, *54*, W04501.
55. Paz, A.R.D.; Collischonn, W.; Tucci, C.E.M.; Padovani, C.R. Large-scale modelling of channel flow and floodplain inundation dynamics and its application to the Pantanal (Brazil). *Hydrol. Process.* **2011**, *25*, 1498–1516. [[CrossRef](#)]
56. Neal, J.; Schumann, G.J.-P.; Bates, P.D. A simple model for simulating river hydraulics and floodplain inundation over large and data sparse areas. *Water Resour. Res.* **2012**, *48*, W11506. [[CrossRef](#)]
57. Pappenberger, F.; Dutra, E.; Wetterhall, F.; Cloke, H.L. Deriving global flood hazard maps of fluvial floods through a physical model cascade. *Hydrol. Earth Syst. Sci. Discuss.* **2012**, *9*, 6615–6647. [[CrossRef](#)]
58. Westerhoff, R.S.; Kleuskens, M.P.H.; Winsemius, H.C.; Huizinga, H.J. Automated global water mapping based on wide-swath orbital synthetic aperture radar. *Hydrol. Earth Syst. Sci.* **2013**, *17*, 651–663. [[CrossRef](#)]
59. Tian, J.; Tian, F.; Li, T.; Sun, Q.; Li, X. Mountain ditch dam-break flood risk analysis based on fusion technology of GIS and hydrodynamic model. *Water Resour. Power* **2018**, *36*, 64–67. (In Chinese)
60. Wang, L. Flood Simulation and Optimization Study on Risk Aversion Transfers in Flood Control Protected Zone Based on GIS. Master's Thesis, Tianjin University, Tianjing, China, 2015. (In Chinese)
61. Zhang, N. The Flood Risk Analysis of the Dam Break and Overflow Floods in Ningxia Section under the Encounter of Floods in Mainstream and Its Tributaries. Master's Thesis, Tianjin University, Tianjing, China, 2015. (In Chinese)
62. Hu, C. Changes in runoff and sediment loads of the Yellow River and its management strategies. *J. Hydroelectr. Eng.* **2016**, *35*, 1–11. (In Chinese)

63. Yuan, X.; Tian, F.; Wang, X.; Chen, M.T. Small-scale sediment scouring and siltation laws in the evolution trends of fluvial facies in the Ningxia Plain Reaches of the Yellow River (NPRYR). *Quat. Int.* **2018**, *476*, 14–25. [[CrossRef](#)]
64. Fan, X.; Shi, C.; Zhou, Y.; Du, J. Characteristics of flood regime in Ningxia-Inner Mongolia Reaches of the Upper Yellow River. *Resour. Sci.* **2012**, *34*, 65–73. (In Chinese)
65. Zhang, S.; Wang, J.; Pan, Y. Researches of the Yellow River farm land reserve resources in Henan Province based on remote sensing and GIS technology. *Areal Res. Dev.* **2008**, *27*, 120–123. (In Chinese)
66. Bi, J.; Huang, H.; Liu, Y. Flood trace extraction and flood inundation estimation using remote sensing and GIS. *Remote Sens. Inf.* **2016**, *31*, 147–152. (In Chinese)
67. Wang, X.; Ling, H.; Wang, Y.; Zhong, D.; Zhang, H. Analysis on the 2012 flood in Ningxia Section of the Yellow River. *Yellow River* **2014**, *36*, 31–33. (In Chinese)
68. Yue, Z.; Ma, X. Flow profile of the Ningxia Reach in the Yellow River with 2012 flood. *J. Sediment Res.* **2016**, *1*, 47–51. (In Chinese)
69. Ningxia Water Conservancy. *Study on the Management System of the Real-Time Dynamic Flood Risk Mapping in the Ningxia Reach of the Upper Yellow River from Xiaheyuan to Shizuishan*; Ningxia Water Conservancy: Yinchuan, China, 2016. (In Chinese)
70. Hou, Z.; Guo, Y.; Li, Y. Impact of overbank flood study on the bank deposit main channel erosion and the flooded risk in the Lower Reaches of the Yellow River. *Yellow River* **2016**, *38*, 45–47. (In Chinese)
71. Zhang, M.; Huang, H.; Zhang, X. A study of the characteristics of sedimentation in the Lower Yellow River during overbank floods. *Adv. Water Sci.* **2016**, *27*, 165–175. (In Chinese)
72. Zhang, B.; Wang, W. Analysis on the flood control and disaster reduction in the lower Yellow River beach area. *China Water Resour.* **2007**, *17*, 43–46. (In Chinese)
73. Huo, F.; Lan, H. Study of mitigation measures and analysis of flood risk at floodplain in the Yellow River downstream. *Water Conserv. Sci. Technol. Econ.* **2009**, *15*, 135–137. (In Chinese)



© 2019 by the authors. Licensee MDPI, Basel, Switzerland. This article is an open access article distributed under the terms and conditions of the Creative Commons Attribution (CC BY) license (<http://creativecommons.org/licenses/by/4.0/>).